

Shubnikov–de Haas oscillations in a nonplanar two-dimensional electron gas

G M Gusev[†], A A Quivy[†], J R Leite[†], A A Bykov[‡], N T Moshegov[‡],
V M Kudryashev[‡], A I Toropov[‡] and Yu V Nastaushev[‡]

[†] Instituto de Física da Universidade de São Paulo, CP 66318, CEP 05315-970, São Paulo, SP, Brazil

[‡] Institute of Semiconductor Physics, Russian Academy of Sciences, Siberian Division, Novosibirsk, Russia

Sunrise Setting

Marked Proof

SST/101328/PAP

17346ap

Printed on 15/10/99

at 11.42

Received 25 January 1999, in final form 13 September 1999, accepted for publication 24 September 1999

Abstract. We have measured the Shubnikov–de Haas (SdH) oscillations of a nonplanar two-dimensional electron gas (2DEG) fabricated by overgrowth of a GaAs/AlGaAs heterojunction on a pre-patterned substrate. When placed in a uniform external magnetic field B , the field normal to the nonplanar 2DEG is spatially modulated, and electrons experience a nonuniform magnetic field. In a tilted magnetic field, the SdH oscillations are much more strongly damped than in a field perpendicular to the substrate. We consider several mechanisms which may be responsible for the anomalous behaviour of the SdH oscillations in the tilted magnetic field. We conclude that the electron scattering by the magnetic field spatial fluctuations plays a main role in the transport properties of a nonplanar 2DEG at low magnetic field. An analysis of the Shubnikov–de Haas oscillations in a tilted magnetic field provides a new method to study the surface profile of a nonplanar heterostructure containing a 2DEG.

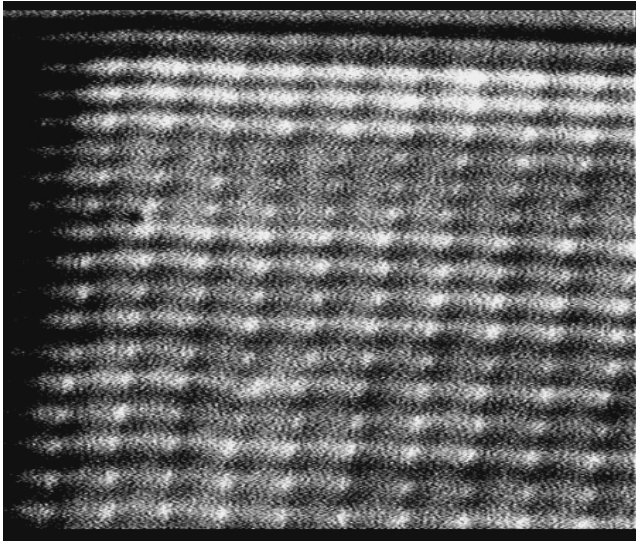
Recently, new regrowth techniques have been reported to produce a two-dimensional electron gas (2DEG) on nonplanar pre-patterned GaAs substrates [1, 2]. In [1] a nonplanar 2DEG was fabricated by molecular beam epitaxy (MBE) growth of GaAs/AlGaAs heterostructures on a wafer pre-patterned with a single facet at an angle of 20° to the surface and an over $1 \mu\text{m}$ wide etched ridge. A 2DEG with mobility $245\,000 \text{ cm}^2 \text{ V}^{-1} \text{ s}^{-1}$ at $T = 4.2 \text{ K}$ and carrier density $n_s = 4.8 \times 10^{11} \text{ cm}^{-2}$ was fabricated. In [2] a 2DEG was grown also employing MBE overgrowth of GaAs/AlGaAs on the wafer which was etched to produce a periodic lattice of holes with submicron diameter (antidots). The mobility of the regrown 2DEG was $70 \times 10^3 \text{ cm}^2 \text{ V}^{-1} \text{ s}^{-1}$ at a concentration of $5.5 \times 10^{11} \text{ cm}^{-2}$. The interest in fabricating such systems is generated by the possibility of investigating the effects of varying the topography of an electron gas. On the other hand nonplanar 2D systems allow us to study the physics of electron motion in a nonuniform magnetic field. Since a 2DEG is sensitive to only the normal component of the magnetic field B , electrons confined to a nonplanar heterojunction experience nonuniform magnetic field varying with position, depending on the surface shape, if a uniform B is applied to such a nonplanar surface.

This paper reports on the fabrication of a 2DEG on a nonplanar stripe-shaped surface with small heights of the stripes. The 2DEG has the mobility of $(250\text{--}400) \times 10^3 \text{ cm}^2 \text{ V}^{-1} \text{ s}^{-1}$ at a carrier density of $5.4 \times 10^{11} \text{ cm}^{-2}$.

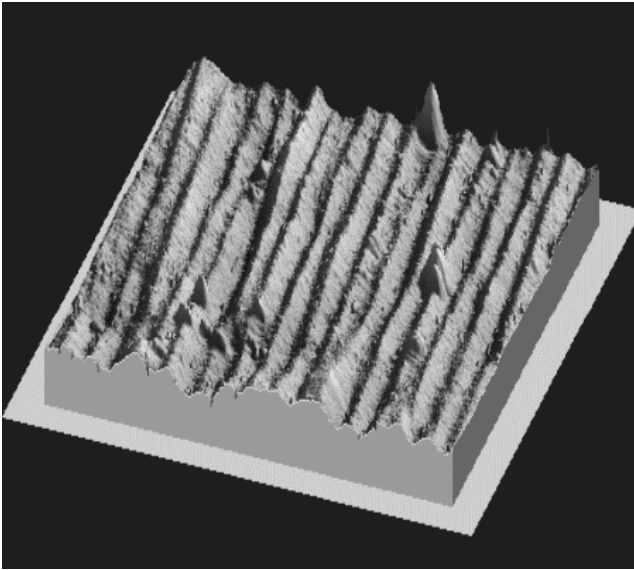
We studied the electron transport properties of nonplanar 2D electrons in a magnetic field.

Samples were fabricated employing overgrowth of GaAs and AlGaAs materials by MBE on pre-patterned (100) GaAs substrates. The pre-patterning consists of a lattice (periodicity $d = 0.7 \mu\text{m}$) of holes (diameter $0.35 \mu\text{m}$) made by electron lithography. The holes have been etched with an $\text{H}_2\text{SO}_4\text{--H}_2\text{O}_2\text{--H}_2\text{O}$ (1:1:1) solution to a depth of $0.3 \mu\text{m}$. The etchant employed has been shown to etch GaAs anisotropically, therefore the (111)A planes been approximately exposed on the hole side wall in the $(1\bar{1}0)$ direction. The same etchant results in a shallow and smoother structure on the hole wall side in the orthogonal $(0\bar{1}1)$ direction. The substrate was then transferred into the MBE growth chamber and heated to 560°C for 12 h. A HEMT structure was grown on the cleaned surface at 600°C . The growth consisted of a 100 nm GaAs buffer layer, a 20 period superlattice with 2 nm AlAs and 5 nm GaAs, 800 nm of GaAs, 20 nm of AlGaAs, a δ -doped Si sheet (10^{12} cm^{-2}), 40 nm of AlGaAs, a second δ -doped Si sheet ($2.8 \times 10^{11} \text{ cm}^{-2}$) and 100 nm of AlAs followed by an Si-doped (10^{18} cm^{-3}) GaAs cap layer.

Figure 1(a) shows a scanning electron microscope (SEM) image of the etched surface prior to growth. Because of the anisotropic wet etching, the holes were elliptically shaped. The thick ($0.8 \mu\text{m}$) GaAs buffer layer was grown to smooth out any steps in the crystal planes, and rapid



(a)



(b)

Figure 1. (a) SEM image of a sample prior to the growth and (b) $10\ \mu\text{m} \times 10\ \mu\text{m}$ AFM image of the same sample as in (a) after regrowth.

planarization of the initial surface did not allow us to see any corrugation in the SEM image of the structured surface taken after regrowth. Figure 1(b) shows an atomic force microscopy (AFM) image of such a surface. The scan is $10\ \mu\text{m} \times 10\ \mu\text{m}$ wide and was realized in contact mode. The significant mobility of GaAs atoms on the different facets leads to a fast planarization of the surface and creation of a new (100) plane [3,4]. Because the initial surface has shallow and smooth steps in the $(01\bar{1})$ direction, after regrowth the corrugation amplitude is much smaller than in $(1\bar{1}0)$ directions, when the surface was preferentially etched. This leads to a stripe-like structure of the overgrown surface. Because the 2DEG is buried close to the surface, it has the same shape. We should note that in work [2] ‘dimpled’ surface structure was obtained from an initially antidot patterned substrate. We believe that the growth is very sensitive to a small variation of substrate etching, which was not controlled in [2]. Figure 2(a) shows the profile of

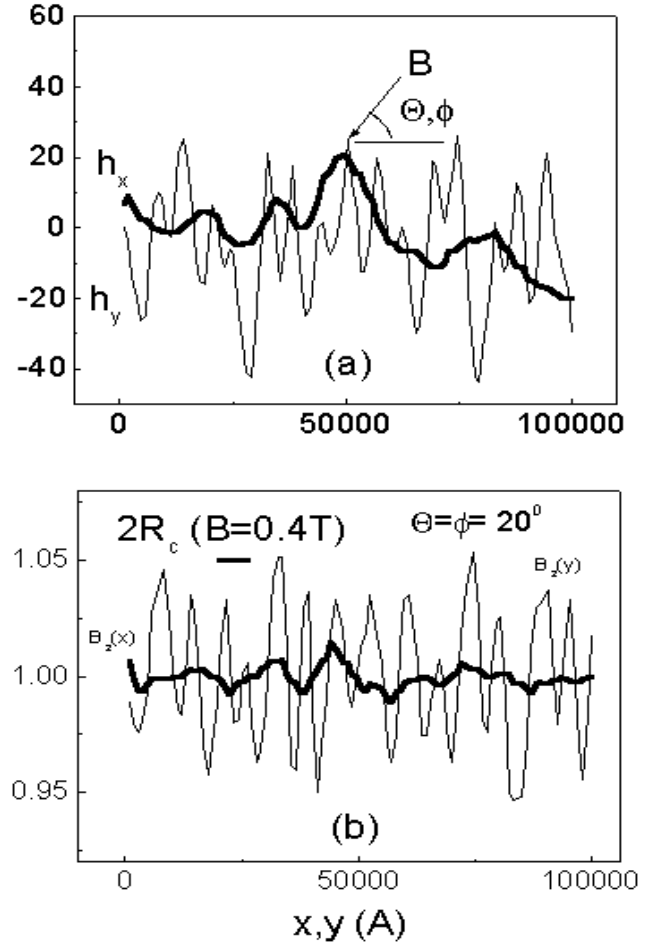


Figure 2. (a) Profile of the surface along the x and y direction of the sample shown in figure 1(b). (b) Magnetic-field profile calculated for the surface profile shown in (a) when the magnetic field is tilted in the x (thick line) or y (thin line) direction. Bars—cyclotron diameter at 0.4 T.

the surface in the direction along the stripes (x direction) and across the stripes (y direction). Along the x direction we can see both irregular and periodical components in the surface corrugation. The average periodicity is coincident with the antidot lattice periodicity before overgrowth. The corrugation height h varies between 20 and $65\ \text{\AA}$. Figure 2(a) shows also an irregular surface profile along the x direction with smaller corrugation height and larger average periodicity than along the y direction. The origin of these irregularities is not understood. We can only assume that they arise from some small variation of the etching depth. The patterned area was $140 \times 140\ \mu\text{m}^2$. After regrowth, the HEMT structure was processed into Hall bars, and the nonplanar surface was situated on one side of the Hall bar (see inset of figure 3). The distance between the voltage probes was $100\ \mu\text{m}$ and the width of the bar was $50\ \mu\text{m}$. As mentioned before, since a 2DEG is sensitive only to the normal component of B , measuring the resistance for different angles between the field and the normal to the substrate surface allows us to vary the magnitude of the magnetic field fluctuations. If the magnetic field is tilted away from the normal to the substrate, the normal component of B can be expressed as

$$B_N(x, y, z) = (\vec{B} \cdot \vec{\nabla} f) / |\vec{\nabla} f| \quad (1)$$

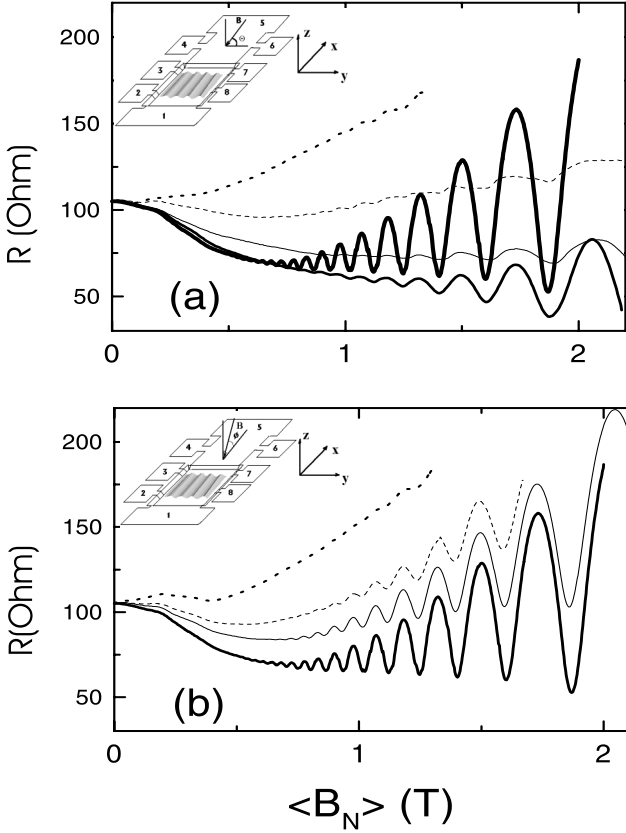


Figure 3. Magnetoresistance as a function of the magnetic field component perpendicular to the substrate for different angles between the applied magnetic field and the normal to the substrate at $T = 1.5$ K. The insets show a schematic view of the experimental geometry. (a) $\theta = 90^\circ$ (thick line), 53° (thick line), 36° (thin line), 20° (dotted line), 10° (dashes). (b) $\theta = 90^\circ$ (thin line), 38° (thick line), 20° (dotted line), 12° (dashes).



where gradient $\bar{\nabla}f$ (df/dx , df/dy , df/dz) is defined for the surface $f(x, y, z) = 0$. In realistic samples we have $df/dy \sim h/d \ll 1$. Therefore, if the external magnetic field is tilted in the y direction, the expression (1) can be rewritten as $B_N \approx B \sin \theta + (df/dy)B \cos \theta \approx \langle B_z \rangle + \delta B(x)$, where θ is the angle between the external magnetic field and the substrate plane; $\langle B_N \rangle = B \sin \theta$ is the average normal component of B . At angles $\theta \gg h/d \approx 1^\circ$, the average magnetic field $\langle B_z \rangle$ is larger than the magnitude of the magnetic field fluctuations $\delta B(x)$. Figure 2(b) shows the magnetic field profile when the external field is tilted in the x or in y direction. When the applied magnetic field is quasi-parallel to the substrate, at an angle $\theta \sim h/d \approx 1^\circ$, the effective magnetic field becomes essentially nonuniform and sign alternating. In this work we considered the case when $\langle B_N \rangle \gg \delta B$. The Hall voltage of the planar 2DEG was used to measure tilt angles with a precision of 1 – 2° . We studied seven samples with identical parameters. The results obtained for one typical specimen are presented in detail. Figure 3(a) shows the longitudinal magnetoresistance for different angles Θ and ϕ between the field and the normal to the substrate plane as a function of the magnetic field component B_N perpendicular to the substrate. The magnetic field was tilted in the y (a) and x direction (b). At a magnetic field ~ 0.4 T, the SdH oscillations are clearly seen. The oscillations are shifted towards higher total field, following,

as expected, a $(\sin \theta)^{-1}$ law. However, as B is tilted from the normal, SdH oscillations are more strongly damped than for the perpendicular field. This damping is much stronger when B is tilted away from the normal in the y direction (a) than in the x direction (b).

In the 2D case, the amplitude of the SdH oscillations is given by [6]:

$$\Delta R/R = (4A_T / \sinh A_T) \exp(-\pi/\omega_c \tau) \cos(2\pi^2 h n_s / eB) \quad (2)$$

where $A_T = 2\pi^2 kT / h\omega_c$; τ is a single-particle relaxation time which is typically 10–100 times smaller than the momentum relaxation time extracted from the mobility measurements at $B = 0$ [7]. Figures 4(a), (b) show the amplitude of the magnetoresistance oscillations as a function of the tilt angles Θ and ϕ , when B is tilted away from the normal, consequently, in the y and x directions, for two values of magnetic field 0.6 and 0.95 T. We should note that in the planar 2DEG the magnitude of SdH oscillations does not change (within the accuracy of 10%). Magnetooscillations in planar heterostructures in the presence of an in-plane magnetic field have been investigated in [8]. A small (3–5%) increase of the effective mass has been found at $\theta = 10^\circ$ due to the distortion of the Fermi contour by the parallel magnetic field. In accordance with equation (2) it leads to a small (3%) increase of the SdH amplitude in a tilted magnetic field, which disagrees with our experimental observations. Therefore, the observed decrease of the SdH amplitude with the angle in our nonplanar samples can be attributed to the fluctuations of magnetic field arising from the surface corrugation, as seen in the AFM image (figures 1(b) and 2(a)).

Several effects can be responsible for the damping of the SdH oscillations in the tilted magnetic field. At small magnetic field the cyclotron diameter $2R_c = 2v_F/\omega_c$ (v_F —Fermi velocity, $\omega_c = eB/mc$ —cyclotron frequency) is larger than the magnetic periodicity. For example, figure 2(b) shows the size of the cyclotron circle at $B = 0.4$ T, when SdH oscillations start to appear. The magnetic field is no longer homogeneous inside the circular orbit, $\langle B_N \rangle$ does not depend on the position of the circle; however the magnetic field fluctuations $\langle \delta B \rangle$ are zero on average. In this case, as has been shown in [9], the second order corrections to the magnetic flux through the cyclotron circle should be taken into account. This leads to the broadening of the Landau level. This broadening can be used to define a single particle relaxation time due to the scattering by magnetic field fluctuations [9]. At high magnetic field the cyclotron diameter becomes smaller than magnetic periodicity. In this case the average magnetic field, and, consequently, the cyclotron energy of the orbits depend on their position. This also leads to the additional broadening of Landau levels and SdH oscillations. Finally, it has been assumed that the damping factor of the SdH oscillations is governed by localization effects [10]. If the magnetic field is strong, the particles can drift along the percolation trajectories with zero $\langle \delta B \rangle$. The number of such trajectories decreases with decreasing B , which also leads to the extremely sharp falloff of the amplitude of the oscillations.

A theoretical model of electron transport in a random short-range and long-range magnetic potential (in the

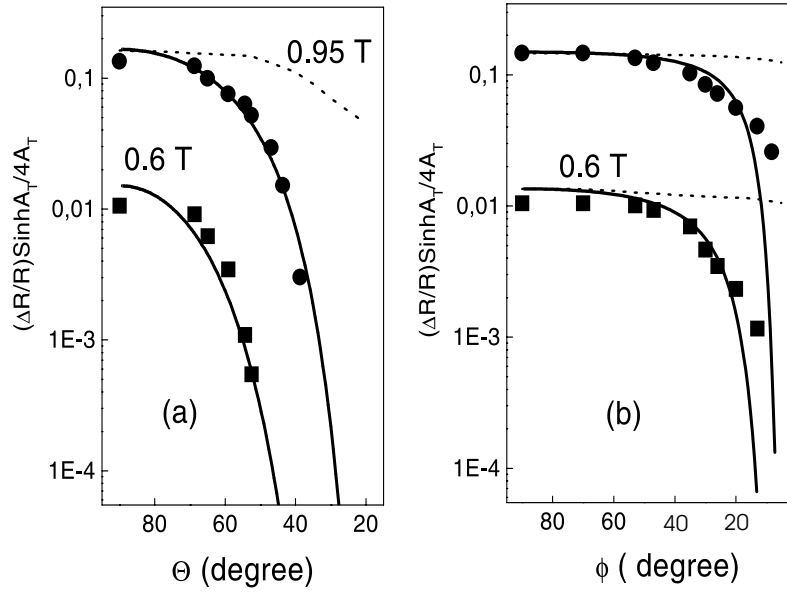


Figure 4. Amplitude of the SdH oscillation at fixed normal component of magnetic field as a function of tilt angle, when magnetic field is tilted in x (a) and y directions (b). Thick lines—equations (3)–(5) calculated for realistic surface profile (figure 2(a)). Dashed lines—equation (2) with position dependent filling factor calculated for realistic surface profile.

presence of additional uniform magnetic field) has been reported in [9]. In contrast to the typical case of an impurity random potential (equation (2)) it was obtained that $\Delta R \sim \exp[-\pi^4/(\omega_c \tau_m)^4]$ when the average periodicity of the magnetic-field fluctuations d is much larger than the cyclotron diameter $2R_c$, and that $\Delta R \sim \exp[-\pi^2/(\omega_c \tau_m)^2]$ for short correlation length $d \ll 2R_c$, where τ_m is a single-particle relaxation time due to the random magnetic field. Because in our case the magnitude of the magnetic field fluctuations is proportional to the external magnetic field (see equation (1)), it leads to dependences $\Delta R \sim \exp[-\pi^2/(\omega_c \tau_m)^2]$ for $d \gg 2R_c$ and $\Delta R \sim \exp[-\pi/(\omega_c \tau_m)]$ for $d \ll 2R_c$. More detailed calculations are presented elsewhere [11]. Taking into account that the impurity electric field and nonuniform magnetic field induce the random phase along the classical paths independently, this leads to the following damping of the SdH oscillations in the presence of impurities and random magnetic potentials [11]:

$$\Delta R \sim \exp[-\pi/(\omega_c \tau_s) - \pi/(\omega_c \tau_m)] \quad (3)$$

$$1/\tau_m = (2\pi^3 m^3 v_F^3 c^3 / e^3 \Phi_0^2) \langle \delta B^2 \rangle / \langle B_N \rangle^3 \quad (4)$$

where $\Phi_0 = hc/e$.

If $d \ll 2R_c$ the averaging reduces the amplitude of the magnetic field fluctuations by a factor $(2R_c/d)^{1/2}$, which is the square root of the number of cells of size d along the cyclotron orbits of length $2R_c$. Substituting equation (1) into formula (4) and taking into account that $\langle \delta B \rangle / \langle B_N \rangle^3 \approx \langle df/dy^2 \rangle (\cot \Theta)^2 (d/2R_c) (1/\langle B_N \rangle)$, we find

$$1/\tau_m \approx \pi (1/\tau_0)^2 (d/v_F) \langle df/dy^2 \rangle (\cot \Theta)^2 \quad (5)$$



where $\tau_0 = h/E_F$ is the characteristic time of the 2DEG. We calculate $1/\tau_m$ for a realistic profile of the surface measured by AFM (figures 2(a), (b)) and substitute it into equation (3) in order to compare our theoretical estimation with experimental results. The single-particle relaxation time

due to impurity scattering $1/\tau_s$ we find from the Dingle plot ($\ln \Delta R/R$ against $1/B$) in perpendicular B , when magnetic fluctuations are very small, and we can neglect magnetic scattering. Figures 4(a), (b) show results of calculations. We see that the theoretical curves fit experimental results very well without any adjustable parameters for both cases, when magnetic fields are tilted in x and y directions. As we mentioned above, when the magnetic field is tilted in the x direction, at $B = 0.6$ T the cyclotron diameter is still larger than the magnetic periodicity, and broadening of the SdH oscillations is due to the magnetic fluctuation scattering. At $B = 0.95$ T we have $2R_c < d$ and for calculation of the magnetic scattering time we should use equation (4). In this case the single-particle time becomes magnetic-field dependent, and it is possible to rewrite equation (3) in the following form:

$$\Delta R \sim \exp[-\pi/(\omega_c \tau_s) - \pi/(\omega_c \tau_m^*)^2]$$

where $1/\tau_m^* = (2\pi)^{1/2} (\langle df/dx \rangle \cot \Theta) / \tau_0$.

When the magnetic field is tilted in the y direction the cyclotron diameter is smaller than the magnetic periodicity even at $B = 0.6$ T, and for comparison of our theoretical model with experimental results we calculate time τ_m using equation (4) (figure 4(b)). If $2R_c < d$ the additional mechanism—broadening due to the spatial fluctuation of the Landau level factor—should be also taken into account. In order to compare this mechanism with experimental results we calculate the amplitude of the SdH oscillations considering a realistic profile of the magnetic field (figure 2(b)). Results of these calculations are shown in figures 4(a), (b) by dashed lines. We see that this effect is smaller than the damping of SdH oscillations due to the magnetic scattering, and we can neglect it. However, we should note that at stronger magnetic field and for smaller tilt angle this inhomogeneous broadening of Landau levels can play an important role. At small angle ϕ the magnetic

field fluctuations are comparable with the normal component of B . This could change the transport mechanism in two dimensions. As we mentioned above, in a sign-alternating field only electrons drifting along $\langle B \rangle = 0$ line can contribute to the conductivity. Theory predicts for long-range magnetic field fluctuations [10]: $\Delta R \sim \exp[-\pi/(\omega_c \tau_m)^8]$, or in our case, because $\delta B \sim B_N$, we have

$$\Delta R \sim \exp[-\pi/(\omega_c \tau_m^*)^4]. \quad (6)$$

We see that this dependence of the SdH oscillation amplitude is extremely sharp, and we do not observe it in the experiment. Further experiments obviously are needed to study the role of the electron localization in the random sign-alternating magnetic field.

From the comparison of our experimental results with theory it follows that the SdH oscillations are more strongly damped when B is tilted in the y direction because of the smoother surface profile in the x direction. Therefore it is possible to use the measurements of the SdH oscillations in the tilted magnetic field for the determination of the parameter df/dx (or df/dy).

In summary, we report the fabrication of a nonplanar stripe-shaped 2DEG with a small amplitude of surface corrugation. By rotating the sample in an external magnetic field, we demonstrate that the nonplanar 2DEG has transport properties which are different from a planar 2DEG. In particular, a strong damping of the SdH oscillations is found in tilted magnetic field. This damping arises from the additional electron scattering by a nonuniform magnetic field. The damping of the SdH oscillations is different when the magnetic field is tilted away from the normal to the surface in the directions $\langle 1\bar{1}0 \rangle$ and $\langle 01\bar{1} \rangle$. This is consistent with the measurements of the surface profile by atomic force microscope.

Acknowledgments

The authors thank E Mucciolo for valuable discussions and Professor M A Cotta for allowing access to the AFM. The work was supported by the RFFI grant No 97-02-18402-a and FAPESP grant N97/03355-0 and CNPq (Brazilian agencies).

References

- [1] Leadbeater M L, Foden C L, Burroughes J H, Pepper M, Burke T M, Wang L L, Grimshaw M P and Ritchie D A 1995 *Phys. Rev. B* **52** R8628
- [2] Gusev G M, Gennser U, Kleber X, Maude D K, Portal J C, Lubyshev D I, Basmaji P, Silva M de P A, Rossi J C and Nastaushev Yu V 1996 *Surf. Sci.* **361/362** 855
- [3] Turgo F S, Simhony S, Kash K, Hwang D M, Ravi T S, Kapon E and Tamargo M C 1990 *J. Cryst. Growth* **104** 766
- [4] Kapon E 1994 *Epitaxial Microstructures, Semiconductors and Semimetals* vol 40, ed A C Gossard (New York: Academic) p 259
- [5] Arnone D D, Cina S, Burroughes J H, Holmes S N, Burke T, Hughes H P, Ritchie D A and Pepper M 1997 *Appl. Phys. Lett.* **71** 497
- [6] Ando T 1974 *J. Phys. Soc. Japan* **37** 1233
- [7] Coleridge P T, Stoner R and Fletcher R 1989 *Phys. Rev. B* **39** 1120
- [8] Smreka L, Vasek P, Kolacek J, Jungwirth T and Cukr M 1996 *Surf. Sci.* **361/362** 509
- [9] Aronov A G, Altshuler E, Mirlin A D and Wolfe P 1995 *Europhys. Lett.* **29** 239
- [9] Aronov A G, Altshuler E, Mirlin A D and Wolfe P 1995 *Phys. Rev. B* **52** 4708
- [10] Mirlin A D, Polyakov D G and Wolfe P 1998 *Phys. Rev. Lett.* **80** 2429
- [11] Gusev G M, Leite J R, Bykov A A, Moshegov N T, Kudryashov V M, Toropov I and Nastaushev Yu V 1999 *Phys. Rev. B* **59** 12 567



Annotations from 101328.pdf

Page 3

Annotation 1; Label: EE & SS; Date: 10/15/1999 3:41:42 PM

Author?

thick and thick, please clarify

or

perhaps use thick and very thick

Page 4

Annotation 1; Label: EE & SS; Date: 10/15/1999 11:48:13 AM

Author?

changes OK

Page 5

Annotation 1; Label: EE & SS; Date: 10/15/1999 11:48:48 AM

Author?

Is ref [5] cited, please indicate where